Acknowledgment. We gratefully acknowledge the generous financial support of the National Science Foundation (Grants CHE 7717877 and CHE 8022854) and the Alfred P. Sloan Foundation. The assistance of the NSF Northeast Regional NMR Facility at Yale University, funded by Grant CHE 7916210 from the Chemistry Division, and the Middle Atlantic Mass Spectrometry Laboratory at the Johns Hopkins University School of Medicine is also acknowledged with gratitude.

Characterization of the Silicon–Aluminum Distribution in Synthetic Faujasites by High-Resolution Solid-State ^{29}Si NMR

M. T. Melchior,* D. E. W. Vaughan, and A. J. Jacobson

Contribution from the Exxon Research and Engineering Company, Linden, New Jersey 07036.
Received August 17, 1981

Abstract: Silicon-29 NMR spectra were obtained at 11.9 MHz by using magic angle spinning and proton dipolar decoupling for a series of 14 synthetic faujasite zeolites. The isotropic ^{29}Si chemical shifts fall in the range −80 to −110 ppm (vs. Me_4Si) reported for four-coordinate silicon in solid silicates and aluminosilicates. Within this range, a regular paramagnetic shift is observed that correlates with the number (0–4) of aluminum neighbors surrounding silicon. As a consequence of the aluminum neighbor effect, the ^{29}Si NMR spectrum of a typical faujasite consists of up to five lines, the intensities of which reflect the distribution of silicon among sites having 0–4 aluminum neighbors. The details of these distributions provide evidence for a high degree of ordering in the faujasite lattice. We find that the Si,Al distribution is consistent with Lowenstein's rule, which excludes Al–O–Al linkages. Further, for a given Si/Al ratio the detailed distribution can be calculated by considering the faujasite lattice as a narrow distribution of ordered structures which minimize Al–O–Si–O–Al linkages.

Faujasite is a naturally occurring zeolite that can be readily synthesized under mild laboratory conditions over a range of Si/Al ratios. Synthetic sodium faujasites with Si/Al ratios between 1.0 and 1.5 and between 1.5 and 3.0 are conventionally called X and Y zeolites,[1,2] respectively. In practice, sodium faujasites with Si/Al ratios greater than 2.7 are difficult to obtain by direct synthesis. Directly synthesized faujasites should be distinguished from materials made by chemical dealumination of lower Si/Al compositions. Such high silica compositions are known as "stabilized" or "ultrastable" faujasites.[3] Because of the widespread use of X and Y zeolites as catalysts and sorbents, their structures have been extensively investigated by X-ray diffraction[4] and infrared spectroscopy.[5]

The structure of faujasite is illustrated in Figure 1. The structure, like that of all zeolites, is built up of SiO_4 and AlO_4 tetrahedra linked by corner sharing. Twenty-four such tetrahedra are joined to form a cubooctahedron or sodalite cage, and these secondary units are stacked tetrahedrally to form a cubic diamond lattice. The sodalite cages are joined tetrahedrally through four of the eight hexagonal faces to give hexagonal prisms. Two such sodalite cages are shown in Figure 1 together with the arrangement of atoms around the large central cavity in the structure; oxygens are omitted for clarity.

Despite an impressive body of information concerning the framework structure and the location of cations within it, the distribution of Si and Al among the framework tetrahedral sites is not generally known. The fundamental question concerns the extent of Si,Al ordering and its dependence on composition. Dempsey[6,7] calculated the Madelung energies for different ordered arrangements of Si and Al at Si/Al = 2, and some experimental evidence has been presented to support his conclusions. This evidence is based on discontinuities in the linear correlation between unit cell dimension and the aluminum content of the framework in synthetic sodium faujasites.[8] These discontinuities near Si/Al ratios of 1.4 and 2.0 are small and had not been detected in previous work on sodium Si/Al faujasites[9,10] but were later convincingly demonstrated for Ga-substituted materials.[11] A subsequent X-ray structure determination of a single crystal of zeolite X (Si/Al = 1.18)[12] showed Si,Al ordering in accordance with Loewenstein's rule,[13] which requires a regular alternation of Si and Al in the limit of Si/Al → 1.0. At high silicon content, however, it has often been assumed that Si and Al are randomly distributed among the framework tetrahedral sites.[14]

High-resolution solid-state ^{29}Si NMR spectroscopy has been shown to be sensitive to the distribution of Si and Al in solid aluminosilicates.[15,16] The technique has been applied to zeolite A.[17,18] The NMR data indicate that Si and Al are ordered in zeolite A but suggest that each silicon has three aluminum nearest neighbors in violation of Loewenstein's rule. This unusual ordered structure was subsequently confirmed by neutron diffraction.[19]

(1) Milton, R. M. U.S. Patent 2882244, 1959.
(2) Breck, D. W. U.S. Patent 3130007, 1964.
(3) McDaniel, C. V.; Maher, P. K. In "Zeolite Chemistry and Catalysis"; Rabo, J. A., Ed.; American Chemical Society: Washington, DC, 1967; ACS Monogr. No. 171, pp 285–331.
(4) Smith, J. V. In "Zeolite Chemistry and Catalysis"; Rabo, J. A., Ed.; American Chemical Society: Washington, DC, 1979; ACS Monogr. No. 171, pp 3–79.
(5) Ward, J. W. In "Zeolite Chemistry and Catalysis"; Rabo, J. A., Ed.; American Chemical Society; Washington, DC, 1976; ACS Monogr. No. 171, 118–284.
(6) Dempsey, E. "Molecular Sieves"; Barrer, R. M., Ed.; Society of the Chemical Industry: London, 1968; pp 293–303.
(7) Dempsey, E. *J. Phys. Chem.* **1969**, *73*, 3660–3668.
(8) Dempsey, E.; Kuhl, G. H.; Olson, D. H. *J. Phys. Chem.* **1969**, *73*, 387–390.
(9) Breck, D. W.; Flanigen, E. M. "Molecular Sieves"; Barrer, R. M., Ed.; Society of the Chemical Industry: London 1968; pp 47–61.
(10) Wright, A. C. Rupert, J. P.; Granquist, W. J. *Am. Mineral.* **1968**, *53*, 1293–1303.
(11) Kuhl, G. H. In "Molecular Sieve Zeolites-1"; Flanigen, E. M., Sand, L. B., Eds.; American Chemical Society: Washington, DC, 1971; Adv. *Chem. Ser.* No. 101, p 199.
(12) Olson, D. H. *J. Phys. Chem.* **1970**, *74*, 2758–2764.
(13) Loewenstein, W. *Am. Mineral.* **1954**, *39*, 92–96.
(14) Smith, J. V. In "Molecular Sieve Zeolites-1"; Flanigen, E. M., Sand, L. B., Eds.; American Chemical Society: Washington, DC 1971; 171–197.
(15) Lippmaa, E. T.; Alla, M. A. Pehk, T. J.; Engelhardt, G. *J. Am. Chem. Soc.* **1978**, *100*, 1929–1931.
(16) Lippmaa, E.; Magi, M.; Samoson, A.; Engelhardt, G.; Grimmer, A.-R. *J. Am. Chem. Soc.* **1980**, *102*, 4889–4893.
(17) Engelhardt, G.; Zeigan, D.; Lippmaa, E.; Magi, M. *Z. Anorg. Allg. Chem.* **1980**, *468*, 35–38.
(18) Thomas, J. M.; Bursill, L. A.; Lodge, E. A.; Cheetham, A. K.; Fyfe, C. A. *J. Chem. Soc., Chem. Commun.* **1981**, 276–277.

0002-7863/82/1504-4859$01.25/0

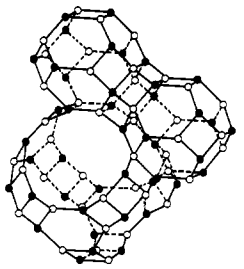

Figure 1. Part of the structure of faujasite with Si/Al = 1 showing two sodalite cages connected by a hexagonal prism and the arrangement of atoms around the large cavity. Oxygens are omitted, solid circles are Al, and open circles are Si.

More recently, Klinowski et al.[20] reported a single silicon resonance in a pure SiO_2 faujasite prepared by dealumination and four-line spectrum arising from silicons with 3, 2, 1, and 0 aluminum neighbors for a synthetic sodium faujasite with Si/Al = 3.06. In this paper, we describe results of a ^{29}Si NMR study of synthetic sodium faujasites in the X and Y composition range. The data show a high degree of Si/Al ordering over the entire composition range investigated. While this manuscript was in preparation, two similar studies of ordering in X and Y zeolites have been reported.[21] Our data and interpretation, however, are substantially different except at the high values of Si/Al (≥2.0), where there is good agreement with both the published experimental work[21] and theoretical calculations.[6,7]

Experimental Section

Eleven sodium faujasites were synthesized in the Si/Al range between 1.27 and 2.63 by using published methods in seeded[22,23] and nonseeded[1,2] synthesis compositions. Three additional samples were obtained from ASTM Committee D32; two of these were prepared by Union Carbide (ASTM 1 and 2) and one by W. R. Grace (ASTM 6). Samples were characterized by X-ray powder diffraction and by BET surface area measurements. All samples showed a single crystalline faujasite phase and had surface areas close to 800 m^2/g. Chemical compositions were determined by plasma spectrometry with a Jarrel-Ash Atomcomp III inductively coupled plasma spectrometer.[24] Lattice parameter measurements were made with a Philips X-ray diffractometer. The correlation between the unit cell constant and the Si/Al ratio determined by chemical analysis was in good agreement with previous data.[8]

Silicon-29 NMR spectra were obtained at 11.85 MHz on a JEOL FX60QS by using the combined techniques of magic-angle spinning and proton dipolar decoupling. Proton dipolar decoupling was found to have little or no effect on the spectra of these materials in which the only protons are due to hydration. The mobility of the water effectively removes any static ^1H–^{29}Si dipolar interaction and precludes use of cross-polarization. Direct pulsed FT NMR excitation was used throughout, employing 90° observing pulses with a pulse repetition time of 4–16 s. Spin–lattice relaxation time measurements on selected samples indicated that this repetition time (>4 s) was sufficient to ensure quantitatively reliable intensities. The spectra displayed in Figures 2 and 8 were obtained by using an apodization function which truncated the free induction decay (FID) at 128 ms, but *without* the use of an exponential weighting function for sensitivity or resolution enhancement. Resolution enhancement is avoided to minimize the possibility of intensity distortions. The chemical shift measurements reported in Table I were obtained *with* resolution enhancement for better definition of peak positions. Under extreme resolution enhancement a further partially resolved splitting, presumably related to next nearest neighbors, could be discerned in some samples. Spectra shown are the resultant of 4–16K FID accumulations. Chemical shifts were referenced to external sodium 4,4-dimethyl-4-silapentanesulfonate (DDS), taken to have a ^{29}Si chemical shift of −1.30 ppm vs. tetramethylsilane. All samples were equilibrated with water vapor before performing NMR experiments. Measurements made on dehydrated samples gave poorly resolved spectra in which the fine structure due to the aluminum neighbor distribution is obscured. We presume this broadening to be due to unresolved chemical shift contributions from cations that are fixed in dehydrated faujasites but undergo rapid site exchange in hydrated samples.

Table I. Chemical Shifts (ppm vs. Me_4Si) for Na Faujasites

sample	Si/Al (anal)	Si/Al (NMR)	number of Al neighbors 4	3	2	1	0
1	1.27	1.26	−86.5	−90.5	−95.2	−100.0	−103.9
2[b]	1.33	1.32	−85.4	−89.8	−94.6	−99.2	−103.0
3	1.50	1.50	−86.0	−90.3	−93.9	−98.9	
4	1.53	1.40	−84.9	−89.3	−93.4	−98.5	
5	1.82	1.75	−85.2	−89.6	−94.4	−99.3	
6	2.41[a]	2.00		−89.6	−94.4	−99.7	
7	2.16	2.31		−89.5	−94.7	−100.0	
8	2.24	2.22		−90.0	−95.1	−100.3	−106.2
9[b]	2.39	2.52		−89.0	−94.1	−99.3	−104.8
10	2.49	2.50		−89.4	−94.6	−99.7	−105.5
11	2.52	2.67		−89.0	−94.2	−99.3	−104.7
12	2.52	2.70			−95.7	−100.5	−105.7
13[b]	2.53	2.64		−90.5	−95.2	−100.5	
14	2.62	2.66		−90.1	−95.2	−100.8	−106.4

[a] Chemical analysis overestimates framework composition because this sample contained amorphous SiO_2. [b] Samples 2, 9, and 13 are ASTM 2, 1, and 6, respectively.

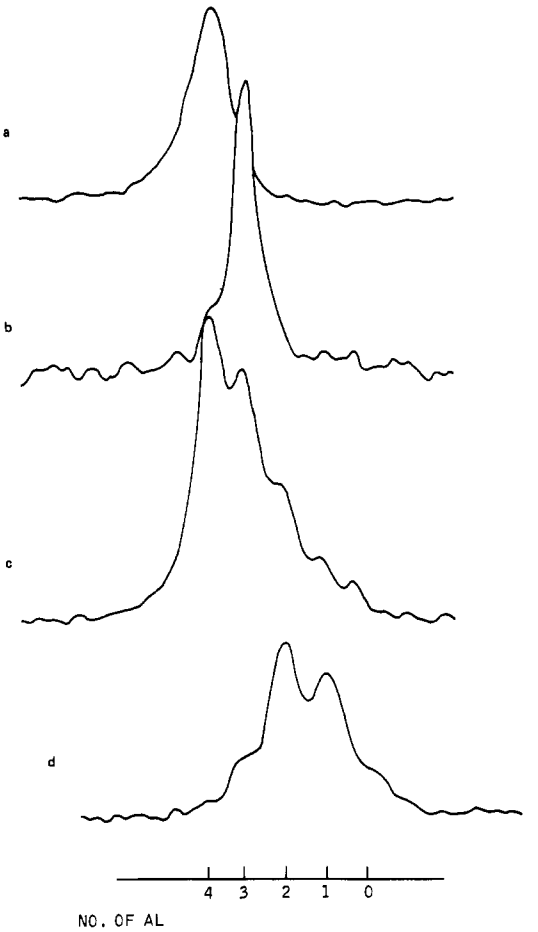

Figure 2. ^{29}Si NMR spectra for (a) sodalite, (b) NaA, (c) NaX, and (d) NaY. Sodalite and NaA have Si/Al = 1.0, NaX and NaY have Si/Al = 1.3 and 2.4, respectively.

Results

The observed ^{29}Si chemical shifts fall in the range −80 to −110 ppm shielded with respect to tetramethylsilane, as previously reported for four-coordinate silicon in solid silicates and aluminosilicates. Within this range, a regular paramagnetic shift is

(19) Bursill, L. A.; Lodge, E. A.; Thomas, J. M.; Cheetham, A. K. *J. Phys. Chem.* **1981**, *85*, 2409–2421.
(20) Klinowski, J.; Thomas, J. M.; Audier, M.; Vasudevan, S.; Fyfe, C. A.; Hartman, J. S. *J. Chem. Soc., Chem. Commun.* **1981**, 570–571.
(21) Ramdas, S.; Thomas, J. M.; Klinowski, J.; Fyfe, C. A.; Hartman, J. S. *Nature (London)* **1981**, *292*, 228–230; Engelhardt, G.; Lippmaa, E.; Magi, M. *J. Chem. Soc., Chem. Commun.* **1981**, 712–713.
(22) Vaughan, D. E. W.; Edwards, G. C.; Barrett, M. G. U.S. Patent 4 178 352, 1979.
(23) Elliott, C. H.; McDaniell, C. V. U.S. Patent 3 639 099, 1979.
(24) Leta, D. P.; Vaughan, D. E. W., to be published.

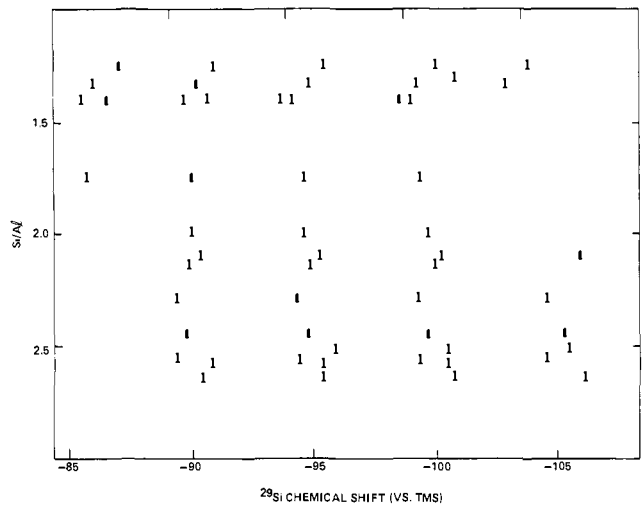

Figure 3. Chemical shift data for 14 sodium faujasites at different Si/Al ratios.

observed that correlates with the number (0–4) of Al neighbors surrounding silicon.[16] In Figure 2, spectra for two faujasites, NaX (Si/Al = 1.3) and NaY (Si/Al = 2.4), are shown together with spectra for sodalite and NaA both with Si/Al = 1.0. As a consequence of the chemical shift due to neighboring aluminums, the ^{29}Si NMR spectra of faujasites consist of up to five absorption lines, the intensities of which reflect the average distribution of Si among sites having 0–4 Al neighbors. Sodalite and NaA, on the other hand, both show single-line spectra indicative of complete ordering at Si/Al = 1. The chemical shift observed for sodalite corresponds to silicon surrounded by four aluminums, Si(4Al), consistent with Loewenstein's rule, whereas NaA was previously reported[17,18] to have the distribution Si(3Al).

The observed chemical shifts for the 14 sodium faujasites investigated are given in Table I together with their compositions determined by chemical analysis and from the NMR spectra (see below). Figure 3 summarizes all of the chemical shift data.

The ^{29}Si NMR spectra fall into three categories for three ranges of the Si/Al ratio (see Figure 3). These ranges correspond to the phase regions discussed by Dempsey et al.[8] For compositions in the X range (Si/Al < 1.4), the NMR spectra consist of five overlapping lines. For compositions in the transition range (1.4 < Si/Al < 2.0), the spectra have four components corresponding to 1–4 Al neighbors. Compositions in the Y range (2 < Si/Al < 3) also have four components, but these correspond to 0–3 Al neighbors. Significantly the NMR spectrum observed at Si/Al = 2.0 has only three components corresponding to 1, 2, and 3 Al neighbors. This overall pattern of distributions is entirely consistent with the sort of Si,Al ordering envisioned by Dempsey.

Before discussing the details of Si,Al ordering as shown by the ^{29}Si NMR spectra, we demonstrate a very simple test of Loewenstein's rule in faujasites. This test depends on the approximate regularity of the observed Al neighbor shift over the entire range of composition as evidenced by Figure 3. If it is assumed that the five Si environments (0–4 Al neighbors) give rise to regularly spaced NMR absorptions of identical width and shape, the first moment (center of mass) of the observed NMR spectrum provides a direct measurement of the average number of Al neighbors per silicon, $\bar{A}$. A plot of $\bar{A}$ measured for 13 of our set of 14 samples vs. the Si/Al ratio R is shown in Figure 4. Figure 4 also shows two theoretical lines. The first is for random distribution of Si and Al in which case the average population of Al adjacent to Si is just the average population overall, i.e., $\bar{A} = 4/(1 + R)$ (random). The second theoretical curve assumes the Loewenstein avoidance rule, which asserts that each Al will be adjacent to four silicon atoms and will contribute 4 to the total number of neighbors of silicon. The average number of Al neighbors is then $\bar{A} = 4(\mathrm{Al/Si}) = 4/R$ (Loewenstein). It is evident from Figure 4 that the Loewenstein curve is in excellent agreement with the observed values. This observation is independent of the details of the

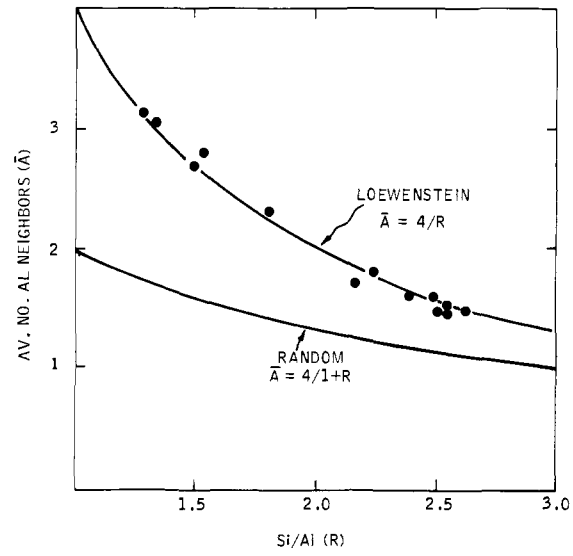

Figure 4. Plot of the average number of Al neighbors silicon ($\bar{A}$) determined by NMR vs. the Si/Al ratio R from chemical analysis. The two theoretical lines are for random Si,Al placement and for distributions subject to Loewenstein's rule.

distributions and merely shows that the Loewenstein rule is a necessary constraint within which countless possible distributions may exist. In the following we take the Loewenstein rule as strictly obeyed for faujasites.

Having established the validity of Loewenstein's rule for faujasites, we can take advantage of the relationship $\bar{A} = 4/R$ to determine R by ^{29}Si NMR spectroscopy. The Si/Al (NMR) ratios in Table I were determined from the measured values of $\bar{A}$. With one exception, the ratios determined from chemical analysis are in good agreement with the NMR results. For sample 6 (not used in Figure 4) the X-ray diffraction data and a broad underlying peak in the NMR spectrum indicated the presence of amorphous SiO_2. The chemical analysis consequently overestimated the framework Si/Al ratio, and the NMR result is more reliable. Lattice parameter measurements support this interpretation.

Discussion

Distribution of Silicon and Aluminum in Isolated Sodalite Cages. To describe the details of the observed ^{29}Si NMR spectra and the Si,Al distributions which they represent, it is useful to classify structures and/or distributions according to a property we have termed *saturation*. A structure is *saturated* if replacement of any Si atom by Al would result in a violation of Loewenstein's rule. The corresponding distribution of Al neighbors (^{29}Si NMR spectrum) is characterized by the absence of a 0-Al component. From Figure 3 and Table I it is evident that the composition range $1.4 < R < 2.0$ is characterized by *saturated* structures whereas compositions outside this range lead to unsaturation.

We now consider specific Si,Al distributions for the sodalite cage of 24 tetrahedral sites. Within a cage each site has three near neighbors; a fourth neighbor results from the incorporation of the sodalite cage into the faujasite framework via four tetrahedrally situated hexagonal prisms. For the moment we focus on the isolated sodalite cage. We assume that for a sodalite cage containing N Al atoms, there is a favored arrangement or, at most, a small number of equally or nearly equally favored arrangements of the N aluminums among the 24 tetrahedral sites. We further assume that the favored arrangement is that which minimizes in order of importance the number of Al–O–Si–O–Al arrangements across 4-rings (ξ_4) and meta arrangements across 6-rings (ξ_6). These assumptions may be thought of as an extension of Loewenstein's rule. The crucial point is that for isolated sodalite cages with $N = 12$, 10, 9, and 8, the arrangements specified by this next nearest neighbor criterion are saturated. For $N = 12$, there is, of course, only a single structure (Figure 5a) that obeys Loewenstein's rule. For $N = 10$ and for $N = 9$, there are two saturated structures at each composition, but the minimum next nearest

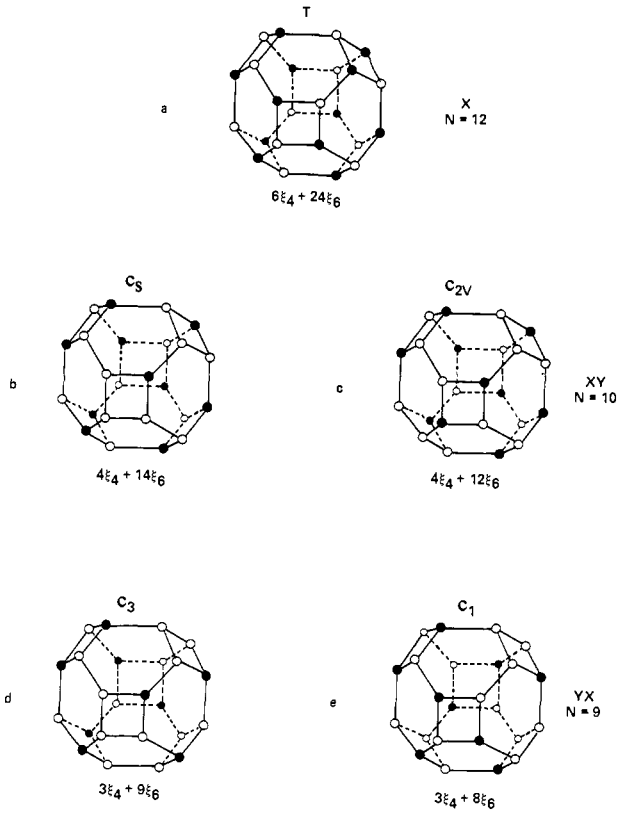

Figure 5. Saturated sodalite cages for $N = 12$, 10, and 9. Solid circles are Al; open circles are Si. The favored arrangements are a, c, and e.

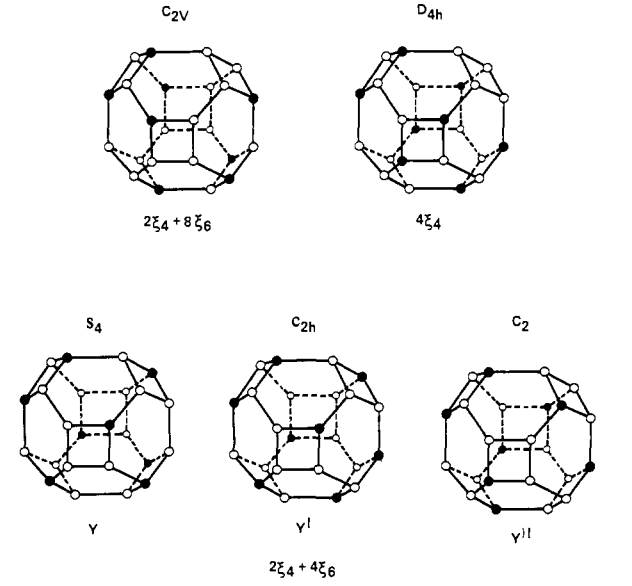

Figure 6. Saturated sodalite cages for $N = 8$. Solid circles are Al; open circles are Si.

neighbor criterion specifies the cage arrangements designated **XY** and **YX**, shown in Figure 5, c and e. For $N = 8$, there are five saturated sodalite cages (shown in Figure 6), three of which have the same combination of next nearest aluminum interactions, two across 4-rings and four across hexagonal faces ($2\xi_4 + 4\xi_6$). One cage has two doubly occupied 4-rings trans and has S_4 symmetry (**Y**). The other two cage arrangements have doubly occupied 4-rings trans with C_{2h} symmetry (**Y'**) and cis with C_2 symmetry (**Y''**). The **Y** cages are the favored arrangements according to the next nearest neighbor criterion. This result agrees with Dempsey's theoretical calculations (see below).

In the following, we consider the faujasite frameworks that can be built using the saturated sodalite cages **X**, **XY**, **YX**, and **Y**. It

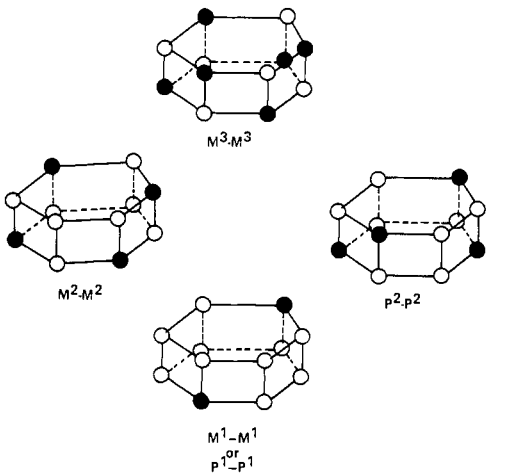

Figure 7. Arrangements of aluminums in the double 6-rings, which preserve the center of charge. Solid circles are Al; open circles are Si.

is interesting to note that each of the three saturated cages **XY**, **YX**, and **Y** selected by the minimum next nearest Al–Al neighbor criterion has four of its eight hexagonal faces with two Al in a para arrangement. For **XY** and **YX** the four para rings are divided between the two sets of tetrahedrally situated hexagonal faces. For **Y** (but not for **Y'** and **Y''**) the four para rings are tetrahedrally situated, as are the four meta rings.

Ordered Distributions of Silicon and Aluminums in Faujasite. Formation of a faujasite lattice involves creation of double 6-rings (hexagonal prisms) by joining sodalite cages on one or the other set of four tetrahedrally situated 6-rings. The four double 6-ring arrangements that are relevant are shown in Figure 7. These arrangements are the only ones that preserve the center of negative charge at the center of the hexagonal prism. Note that the structures for $R < 2$ must involve M^3–M^3 arrangements whereas structures for $R > 2$ must involve the M^1–M^1 or P^1–P^1 arrangement. (The reason for this notation will become evident below.) The M^2–M^2 and P^2–P^2 arrangements are possible over the entire composition range. In counting the Al–Al next nearest neighbors for a faujasite framework, these double 6-rings contribute $3\xi_4$, $1\xi_4$, $1\xi_4$, and $0\xi_4$ per sodalite cage, respectively. Our notation for faujasite frameworks designates which sodalite cage is used (**X**, **XY**, **YX**, or **Y**; see Figures 5 and 6) and the way in which these cages are connected through the double 6-rings (see Figure 7). For example, **XY**($M^3M^3P^2P^2$) denotes a faujasite structure constructed from **XY** sodalite cages connected through two M^3–M^3 and two P^2–P^2 double 6-rings.

It is useful to compare our accounting of Al–Al next nearest neighbors with the results of detailed electrostatic calculations carried out at Si/Al = 2.0.[6] Dempsey considered five structures, two of which correspond to the structures obtained from **Y** by choosing either all M^2–M^2 or all P^2–P^2 double 6-rings. These two structures, which we designate **Y**($M^2M^2M^2M^2$) and **Y**($P^2P^2P^2P^2$), were calculated to have the lowest energy, with **Y**($M^2M^2M^2M^2$) slightly favored. These structures have the same next nearest neighbor count ($6\xi_4 + 4\xi_6$).[25] Significantly higher in energy was the structure based on the D_{4h} cage (Figure 6) with all P^2–P^2 double 6-rings ($8\xi_4$), and higher still the structure based on the C_{2v} cage in Figure 6 with all M^2–M^2 double 6-rings ($6\xi_4 + 8\xi_6$). The fifth structure considered by Dempsey, which had by far the highest electrostatic energy, corresponds to an unsaturated structure based on the **X** cage (Figure 5a) minus four aluminums, **X**($M^2M^2M^2M^2$), and has the greatest next nearest neighbor count ($8\xi_4 + 8\xi_6$). Thus, our heuristic procedure for ranking structures is qualitatively in agreement with the electrostatic calculations. This provides a degree of confidence in our predictions in the cases

(25) It should be noted that each tetrahedral site in the faujasite framework has nine next nearest tetrahedral site neighbors. Two of these are in adjacent sodalite cages across 12-rings and are not included in our accounting.

Table II. Distribution of Aluminum Neighbors for Different Ordered Structures

Si/Al	structure[a]	number of Al neighbors 4	3	2	1	0
12/12	$X(M^3M^3M^3M^3)$	12	0	0	0	0
13/11	$X(M^3M^3M^3M^2)$	8	4	0	0	1
14/10	$XY(M^3M^3P^2P^2)$[b]	4	5	4	1	0
15/9	$YX(M^3P^2P^2P^2)$[b]	2	4.5	6	2.5	0
	$YX(M^3M^2M^2P^2)$[b]	1	6.5	5	2.5	0
16/8	$Y(P^2P^2P^2P^2)$					
	$Y(M^2M^2M^2M^2)$	0	4	8	4	0
	$Y'(M^2M^2P^2P^2)$					
	$Y''(M^2M^2P^2P^2)$[b]	0	3.5	9	3.5	0
17/7	$Y(M^2M^2M^2M^1)$	0	2	8	6	1
	$Y(P^2P^2P^2P^1)$	0	2.5	6	8.5	0
18/6	$Y(M^2M^2M^1M^1)$	0	0	8	8	2
	$Y(P^2P^2PP)$[b]	0	1.5	3.5	11.5	0

[a] The letters refer to the sodalite unit (of Figures 5 and 6) and the superscripted M,P indicate the number and geometry of the Al atoms on the four hexagonal faces in double 6-rings. [b] The two possible choices for building P^2–P^2 double 6-rings (i.e., 1,4-2'5' or 1,4-3'6') are assumed to be equally probable. Two slightly different distributions arise, which have been averaged.

not considered by Dempsey at $N = 10$ (Si/Al = 1.4) and $N = 9$ (Si/Al = 1.67).

Consider now the distribution of Al neighbors about Si predicted for the ordered structures based on the sodalite units **X**, **XY**, **YX**, and **Y**. Each distribution in Table II represents an ordered structure selected as follows. For $N = 12$, the faujasite constructed from the **X** sodalite cage is designated $X(M^3M^3M^3M^3)$. For $N = 11$, the only available sodalite cage is **X** with one Al replaced by Si. This structure we designate $X(M^3M^3M^3M^2)$, an unsaturated structure with one silicon per cage surrounded by four other silicons. For $N = 10$, the framework is built using the **XY** cage and the structure is designated $XY(M^3M^3P^2P^2)$. (It should be noted that formation of a P^2–P^2 double 6-ring always involves a choice between two possibilities, which in general will result in slightly different Al neighbor distributions. We have assumed the two possibilities to be equally probable, since the next nearest neighbor count is unaffected. The half-integral values in some of the Al neighbor distributions in Table II reflect this averaging procedure.) At $N = 9$, even though a single favored sodalite unit is indicated, two frameworks are possible, depending on which set of hexagonal faces is used in forming the double 6-rings. These frameworks, $YX(M^3M^2M^2P^2)$ and $YX(M^3P^2P^2P^2)$, predict quite different Al neighbor distributions. For $N = 8$, there are several possible structures based on the sodalite cages **Y**, **Y'**, and **Y''**. Moreover, there is a choice of two structures even for **Y**, one with P^2–P^2 double 6-rings, the other with M^2–M^2. Those structures based on the **Y** and **Y'** cages have identical Al neighbor distributions, and the other cage, **Y''**, leads to a closely similar distribution. Hence ^{29}Si NMR shows that ordered structures exist at $N = 8$ but cannot distinguish among these possibilities. In order to simplify the following discussion we refer only to the **Y** cage. The discussion including **Y'** and **Y''** becomes rather involved, and omitting them does not affect our conclusions, all of which are consistent with structures based on the **Y** cage.

For the Y range of composition ($N = 7$, $N = 6$), the faujasite structure must be built from sodalite cages which are unsaturated. It is important to note that it is possible to construct a saturated faujasite framework using these unsaturated sodalite units. Consider the two possible frameworks for $N = 8$, which we designate as $Y(M^2M^2M^2M^2)$ and $Y(P^2P^2P^2P^2)$, both formed from the same sodalite unit but in the first case having M^2–M^2 double 6-rings and in the latter case having P^2–P^2 double 6-rings. Now consider the $N = 7$ structures formally related to these, $Y(M^2M^2M^2M^1)$ and $Y(P^2P^2P^2P^1)$. Use of the notation M^1 and P^1 is intended to stress this formal relationship. Both structures contain the double 6-ring arrangement referred to above as M^1–M^1 or P^1–P^1. These two structures have different Al neighbor distributions and in fact $Y(P^2P^2P^2P^1)$ is a saturated framework.

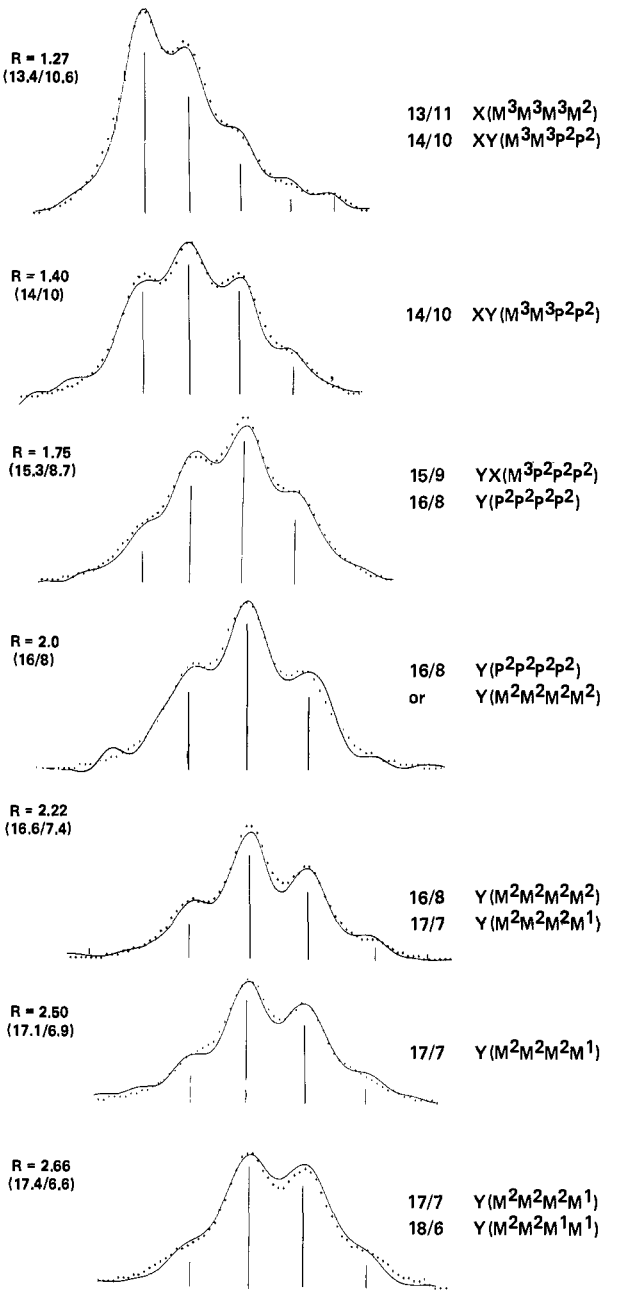

Figure 8. A comparison of the observed ^{29}Si NMR spectra with spectra calculated with distributions taken from Table II. At other than Si/Al = 1.4, 2.0, and 2.4, the spectra have been calculated by interpolation between adjacent values of N.

Similar considerations apply to the $N = 6$ case.

Comparison with Experiment. We find that all of the observed ^{29}Si NMR spectra can be accounted for by using the ordered distributions in Table II. Table II contains all the faujasite structures that can be built from the favored sodalite cages and the double 6-rings shown in Figure 7. The comparison between theory and experiment is shown in Figure 8. The theoretical curves have been constructed by using a basis set of five Lorentzian line shapes of equal width with intensities (shown as solid vertical lines) predicted from distributions taken from Table II. Seven spectra are shown to illustrate the changes in Si/Al ordering with composition. Spectra for the other seven samples show comparable agreement with model.

For compositions corresponding to integral values of N, at $N = 10$ ($R = 1.4$), for example, the NMR spectrum corresponds directly to the distribution in Table II. At intermediate compositions the spectrum is accurately predicted by interpolation between adjacent values of N. Thus at $R = 1.27$ the observed

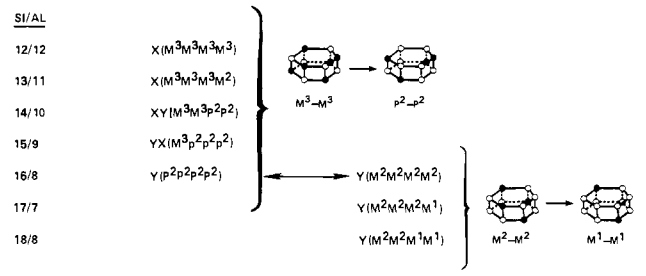

Figure 9. Sequence of ordered structures that show evolution of the Si,Al ordering with increasing Si/Al ratio.

spectrum is reproduced by combining the distributions $\mathbf{X}(M^3M^3M^3M^2)$ and $\mathbf{XY}(M^3M^3P^2P^2)$ in the correct proportions (6:4) to give the measured composition. At $R = 1.76$ it is again necessary to interpolate between two distributions corresponding to $N = 9$ and $N = 8$, but in this case a choice is necessary between the two distributions for $N = 9$, $\mathbf{YX}(M^3M^2M^2P^2)$ and $\mathbf{YX}(M^3P^2P^2P^2)$. The NMR data clearly show that $\mathbf{YX}(M^3P^2P^2P^2)$ is the correct ordered structure. The two possible structures for Y cages at $N = 8$ cannot be distinguished, since both give the same predicted Al neighbor distributions. The three highest Si/Al ratio samples are all correctly predicted from the $N = 8$, 7, and 6 distributions provided the choice is made to join the sodalite cages through M^2–M^2 rather than P^2–P^2 double 6-rings. That this is the correct choice is clearly shown by the spectrum for $R = 2.50$, which corresponds to $N = 7$. A peak corresponding to Si with no aluminum neighbors is observed, which is predicted only for $\mathbf{Y}(M^2M^2M^2M^1)$; i.e., the NMR spectra show clearly that the structure is unsaturated.

Conclusions

We have shown that the observed ^{29}Si NMR spectra for faujasites in the X and Y ranges can be accounted for by a series of ordered structures based on four fundamental sodalite units, **X**, **XY**, **YX**, **Y**. These four cages (Figures 5 and 6) represent fundamentally different Si,Al ordering schemes, each of which predominates over its particular composition range. The four ordered cage arrangements are deduced from a simple hypothesis, which states that for a given Si/Al ratio, the favored Si,Al arrangement is that which minimizes, in order of importance, the number of next nearest neighbor Al,Al pairs across 4-rings and across 6-rings. This hypothesis extends Loewenstein's rule.

It is revealing to consider the formal relationships between the ordered structures that are observed (Figure 9). For $N = 12$ and $N = 11$, all double 6-rings in the faujasite framework have Al atoms in a meta relationship. Formally, the $N = 10$ structure can be thought of as the result of a rearrangement.

$$\mathbf{X}(M^3M^3M^2M^2) \rightarrow \mathbf{XY}(M^3M^3P^2P^2)$$

The overall change in Si,Al ordering involves a conversion of M^3–M^3 double 6-rings to P^2–P^2 double 6-rings. A similar relation between structures holds for $\mathbf{XY}(M^3P^2P^2P^2)$ at $N = 9$ and suggests the end member at $N = 8$ as $\mathbf{Y}(P^2P^2P^2P^2)$. On the other hand the NMR data for Si/Al > 2.0 are consistent with the structures $\mathbf{Y}(M^2M^2M^2M^1)$ and $\mathbf{Y}(M^2M^2M^1M^1)$ at $N = 7$ and 6, respectively. This suggests that the parent member at $N = 8$ is $\mathbf{Y}(M^2M^2M^2M^2)$.

From Figure 9 it can be seen that the progression of structures proposed for increments in N (the number of aluminums per sodalite cage) involves a change in one double 6-ring per two sodalite cages. It is possible to account for intermediate compositions simply by considering larger numbers of sodalite units. Thus we could obtain seven ordered structures between N and $N - 1$ by considering the eight sodalite units in the unit cell. Each of these structures would progressively differ by change in one of the 16 double 6-rings per unit cell. Clearly, it is possible in this way to obtain a quasi-continuous composition variation while maintaining complete Si,Al order.

Finally, we suggest that the reported discontinuity in unit cell dimensions at $R = 2.0$ represents the difference between all P^2–P^2 double 6-rings in $\mathbf{Y}(P^2P^2P^2P^2)$ and all M^2–M^2 double 6-rings in $\mathbf{Y}(M^2M^2M^2M^2)$, the two structures having identical sodalite cage fundamental units.

Note Added in Proof. Since this work was completed, we have obtained data on our samples with improved resolution and sensitivity at a higher ^{29}Si NMR frequency (39.5 MHz). The fine details of these data reveal the presence of more disorder than implied by the model presented here. However, the additional disorder is quite simply taken into account within the framework of our model by considering a somewhat broader distribution of sodalite cage compositions corresponding to a given average composition.

Acknowledgment. We thank D. P. Leta and M. E. Leonowicz for elemental and X-ray analyses, C. F. Pictroski for his assistance in acquiring the NMR spectra, and K. Strohmaier for help with the zeolite synthesis.